Contrib Mineral Petrol (1987) 97:237–250

Contributions to Mineralogy and Petrology
© Springer-Verlag 1987

Transformation of blueschist to greenschist facies rocks as a consequence of fluid infiltration, Sifnos (Cyclades), Greece

Manfred Schliestedt[1] **and Alan Matthews**[2]

[1] Institut für Kristallographie und Petrographie, Universität Hannover, Welfengarten 1, D-3000 Hannover, Federal Republic of Germany
[2] Department of Geology, Institute of Earth Sciences, The Hebrew University, Jerusalem 91904, Israel

Abstract. The transformation from blueschist to greenschist facies forms a major part of the Alpine regional geodynamic evolution of the Cyclades. The transition in metabasic rocks on Sifnos involves the retrogression of eclogites, blueschists and actinolite-bearing rocks from high-pressure conditions which have been estimated at $460 \pm 30°$ C and 15 ± 3 kb. Petrographically observed parageneses are interpreted by a sequence of hydration and carbonation reactions involving the breakdown of omphacite and glaucophane-bearing assemblages to albite + chlorite ± actinolite ± calcite assemblages. The retrograde processes are calculated to occur at pressures of 10 to 8 kb during the isothermal uplift of the Sifnos units. Oxygen isotope analyses of different rock types show that interlayered lithologies have experienced a large degree of isotopic equilibration during both metamorphic phases. However, chemically equivalent rocks show systematic increases in $\delta^{18}O$ from lowest values (~ 8 to 11‰ in metabasics) in the unaltered blueschists in the upper stratigraphic levels to higher values (>15‰ in metabasics) associated with greenschists in the deepest stratigraphic levels. Relict eclogites enclosed within greenschists have the lower $\delta^{18}O$ values typical of unaltered blueschist facies rocks. These isotopic gradients and the $\delta^{13}C$ and $\delta^{18}O$ compositions of carbonates demonstrate an infiltration mechanism involving the upward movement of ^{18}O-enriched fluids whose compositions were buffered by exchange with marble units. Calculated minimum fluid/rock ratios for the blueschist-to-greenschist transition decrease from ~ 0.4 in the deepest studied level (Central Sifnos) and ~ 0.2 in the intermediate level (Kamares Bay samples) to an assumed value of zero in unaltered blueschists. These ratios may be lower if recycling of fluids occurred between schists and marbles. Infiltration of fluids became inhibited as the transformation advanced as a consequence of "sealing effect" of the hydration and carbonation reactions. Although infiltration most probably was a pre-requisite for the regional occurrence of the blueschist-to-greenschist transformation in the Cyclades, the evidence on Sifnos does not suggest the introduction of large quantities of fluid.

Introduction

Concepts of metamorphism have been considerably advanced by evidence that fluid infiltration processes may influence regional metamorphic evolution (e.g., Rumble et al. 1982; Ferry 1983; Graham et al. 1983). Stable isotope studies have been particularly valuable in the identification of the nature and role of the migrating fluid phase because the externally derived fluids may often be in isotopic disequilibrium with the rock units into which infiltration is occurring and bring about clear isotopic signatures of the exchange process (e.g., Bebout and Carlson 1986; Greig et al. 1986; Wickham and Taylor 1985). Our present work concerns the regional metamorphic processes in the Cycladic metamorphic complex (Fig. 1) where studies on Naxos and Sifnos have identified remarkable ^{18}O shifts accompanying fluid infiltration (Rye et al. 1976; Matthews and Schliestedt 1984; Schliestedt et al. 1987).

The Cycladic crystalline complex is an Alpine, collision-type, orogen, whose geological evolution is dominated by three major events: an Eocene (40-45 Ma) high-pressure metamorphism, a low- to medium-pressure metamorphic overprint and a regional scale intrusion of granitoids. The second metamorphism has been dated at between 25-19 Ma (Schliestedt et al. 1987 and references therein) and slightly predated the granitoid igneous activity which continued throughout the Miocene. The metamorphism was dominantly at greenschist facies conditions but occasionally reached amphibolite facies, as in the case of the thermal dome of Naxos, for which Rye et al. (1976) demonstrated the development of large $\delta^{18}O$ gradients between the high-grade migmatitic core and the lower-grade margins.

In contrast to Naxos, where the high-grade overprint almost completely obliterated the earlier high-pressure metamorphism, the metamorphic sequences on Sifnos (Fig. 1) feature excellently preserved high-pressure metamorphic rocks and greenschist facies assemblages. $P-T$ evaluations from oxygen isotope and $Mg-Fe$ exchange thermometry and univariant equilibria show that the high-pressure, blueschist facies, metamorphic assemblages equilibrated at $460 \pm 30°$ C, 15 ± 3 kb, and the greenschist facies assemblages around 400–480° C and 4–7 kb. The resulting broad, clockwise $P-T$ loop suggests that the transition from blueschist to greenschist facies conditions involved a near-isothermal pressure release.

The deepest exposed unit on Sifnos is the largely metabasic Greenschist unit of Central Sifnos (Fig. 1), in which earlier high-pressure assemblages containing glaucophane, omphacite and garnet are almost completely replaced by albite – epidote – chlorite ± calcite ± actinolite assemblages. The high-pressure assemblages are preserved intact in the

---

Offprint requests to: M. Schliestedt

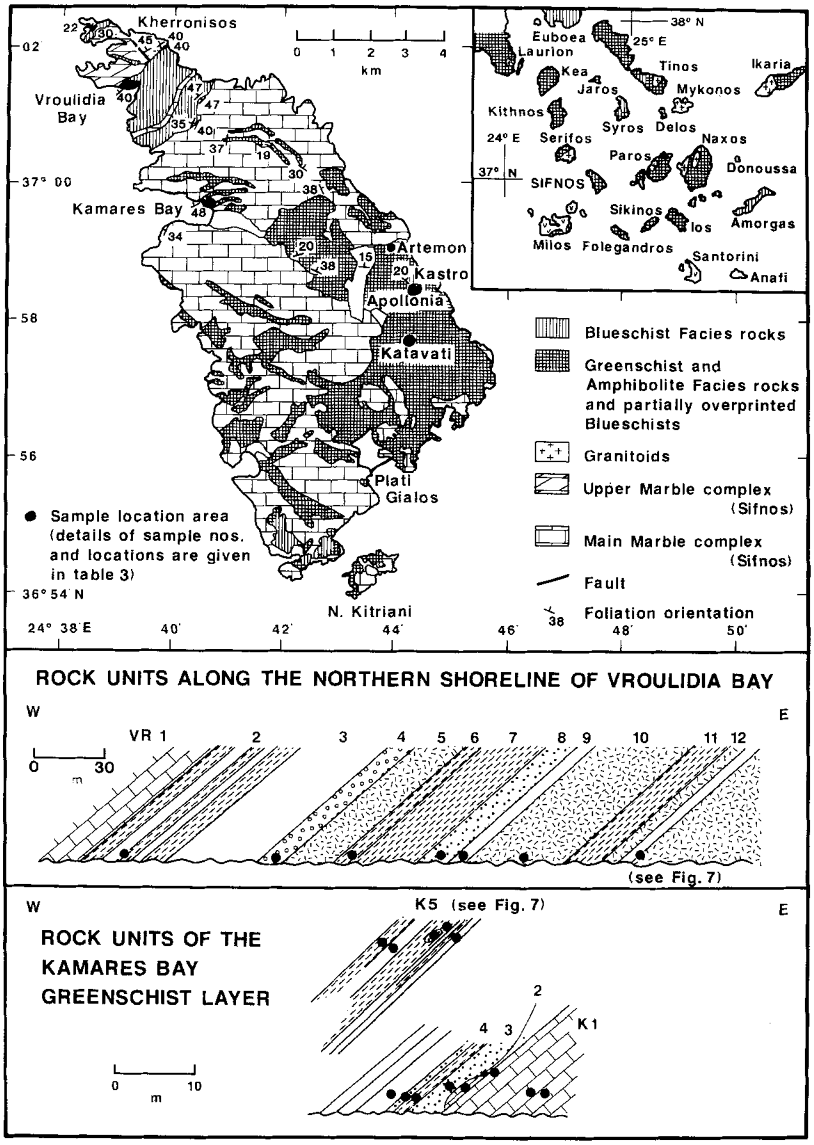

Fig. 1. Geological maps and sections. The *inset map* shows the geological units of the Cyclades. The geological map of Sifnos displays the four main lithological units together with the three main sampling locations: Blueschist Unit (Vroulidia Bay); Greenschist Layer within the Main Marble (Kamares Bay); and the Central Sifnos greenschists (Kastro-Katavati area). The two sections show the interlayered rock units at Vroulidia Bay and Kamares Bay, respectively. *Legend* (Vroulidia Bay units): *VR1* Upper Marble; *VR2* interlayered blueschists and jadeite gneisses (Fig. 2a); *VR3* jadeite gneiss; *VR4* micaschist with calcite lenses; *VR5* coarse eclogite; *VR6* chloritoid-bearing blueschist; *VR7* blueschists with minor eclogite intercalations; *VR8* chlorite-actinolite schist; *VR9* garnet-micaschist: *VR10* eclogite; *VR11* blueschist; *VR12* interlayered eclogites and metasediments. (Kamares Bay units): *K1* Main Marble; *K2* contact zone marble; *K3* micaschist; *K4* and *K5* interlayered sequence of greenschists (containing relict eclogite lenses) with quartz-micaschists and albite gneisses (Fig. 2b)

upper stratigraphic levels as the Blueschist unit of Northern Sifnos (Fig. 1). Separating the Blueschist unit from the Central Sifnos Greenschist unit is a thick marble unit, the Main Marble, consisting of almost pure marbles, with intercalations of schistose rocks exhibiting the greenschist facies overprint in varying degrees.

Indications that fluid infiltration was involved in the blueschist-to-greenschist transition on Sifnos came from the oxygen isotope analyses of minerals for geothermometry (Matthews and Schliestedt 1984). $\delta^{18}O$ analyses of coexisting minerals (e.g., quartz, white mica) from greenschist facies assemblages in Central Sifnos were found to be several per mil heavier than from the same minerals in equivalent rock types of the Blueschist unit. These enrichments led Matthews and Schliestedt (1984) to propose that the blueschist to greenschist facies transformation occurred in the presence of ^{18}O-enriched fluids which infiltrated upwards, but did not penetrate through (because of the impermeability of the Main Marble) to the upper stratigraphic levels where the blueschists were preserved.

The transformation from blueschist to greenschist is a regional process in the Cycladic complex and indeed is most probably typical of Alpine-type orogenic cycles involving a broad clockwise $P-T$ loop. It is clear, therefore, that our understanding of fluid infiltration processes would benefit from a detailed examination of the petrology and stable isotope geochemistry of the blueschist-to-greenschist transformation on Sifnos. To accomplish this we have examined in detail sections at three levels in the Sifnos stratigraphy (Fig. 1): a) the high-pressure, blueschist facies, metamorphic rocks at Vroulidia Bay, b) greenschist facies intercalations within the Main Marble unit at Kamares Bay and c) greenschist facies rocks from Central Sifnos. These three sections, representing upper, intermediate and lower-exposed levels of the Sifnos stratigraphy, are examined for: (1) the isotopic compositional relationships among different interbedded rock types of the same unit, (2) the nature of the blueschist to greenschist facies transition as expressed stratigraphically by the change from complete overprint at the lowest levels to preservation of blueschist facies at upper levels, and (3) the quantities, mechanisms and direction of fluid mobilization. In view of the probable involvement of marbles in the ^{18}O-enrichment of the infiltrating fluids (Matthews and Schliestedt 1984), we have made a comparably detailed study of the carbon and oxygen isotopic geochemistry of carbonate assemblages.

Analytical procedures

Analytical procedures for carbon and oxygen isotope and chemical analyses of whole rocks and minerals have been detailed in Matthews and Schliestedt (1984) and Schliestedt (1986). The chemical analytical data are presented together with modal estimates in Table 1. Oxygen and carbon isotope data are reported in the δ notation in Table 3.

Petrology of the blueschist to greenschist transformation

Field relations

Schematic sections of the lithologies of rock units along the northern shoreline of Vroulidia Bay and the greenschist layer within the Main Marble unit at Kamares Bay are given in Fig. 1.

Units of the Vroulidia Bay blueschist section have been described in detail by Schliestedt (1980, 1986) and Schliestedt and Okrusch (1987). The section is composed of interlayered metabasites (blueschists, eclogites, chlorite–actinolite rocks), meta–acidites (jadeite–quartz gneisses) and metasediments (garnet–micaschists, calcite–epidote schists, quartzites and marbles). The interlayered units dip approximately 40° NW and are concordant with the marbles of the overlying Upper Marble unit (Fig. 1). A particularly notable feature (Fig. 2a) is the repeated interlayering of basic and acidic lithologies on the scale of tens of centimeters (e.g., layers VR 2 and VR 12 in Fig. 1).

The greenschist facies layers at Kamares Bay form part of an ~50 m thick intercalation of silicate rocks, concordantly enclosed within the Main Marble. The lithologies were sampled from the lower contact with the marble to about the centre of the intercalated unit (Fig. 1, bottom). All interlayered rocks display the early NW (~48°) dipping structures, despite the overprint. Equivalent assemblages to those of the Blueschist unit are metabasites: greenschists, meta-acidites: albite gneisses and metasediments: micaschists and quartzites. Field evidence of the transition from blueschist to greenschist facies conditions is provided by the presence of relict eclogite lenses within the greenschist layers (Fig. 2b). At the contact with the Main Marble a 1 m thick marble layer is observed (layer K2). Thin veins of coarse-grained calcite cut across all lithologies. Mesoscopic interlayering of acidic and basic rock layers, similar to that noted above for the blueschists, also occurs in the Kamares section layers K4 and K5 (cf., Fig. 2b).

In contrast to the strongly defined interlayering in the Vroulidia Bay and Kamares Bay sections, the Greenschist unit of Central Sifnos consists mainly of thicker units of metabasic rocks intercalated with metasediments. Sampling was made well within the unit, away from any prominent marble horizon.

Petrology and geochemistry

The Vroulidia Bay Blueschist unit is characterized by a wide variety of mineral assemblages that are typical of the higher grade (garnet–epidote–bearing) parts of the blueschist facies. Depending on the bulk-rock chemistry, typical mineralogies are: (cf., Table 1) epidote + garnet + glaucophane in pelitic metasediments, jadeite + quartz in meta-acidites, garnet + epidote + glaucophane ± chloritoid or omphacite in blueschists and eclogites, and chlorite + actinolite in magnesium-rich metabasites. Figure 3 plots the bulk chemical compositions of all analyzed rocks in an $Al_2O_3 + Fe_2O_3 - FeO + MgO - CaO$ triangle. The various rock types of the Blueschist unit show well defined fields for each type. Schliestedt (1986) has demonstrated that the eclogites, blueschists and actinolite-bearing metabasic rocks represent rocks of different bulk chemical compositions which recrystallized under the same blueschist facies fluid-pressure and temperature conditions.

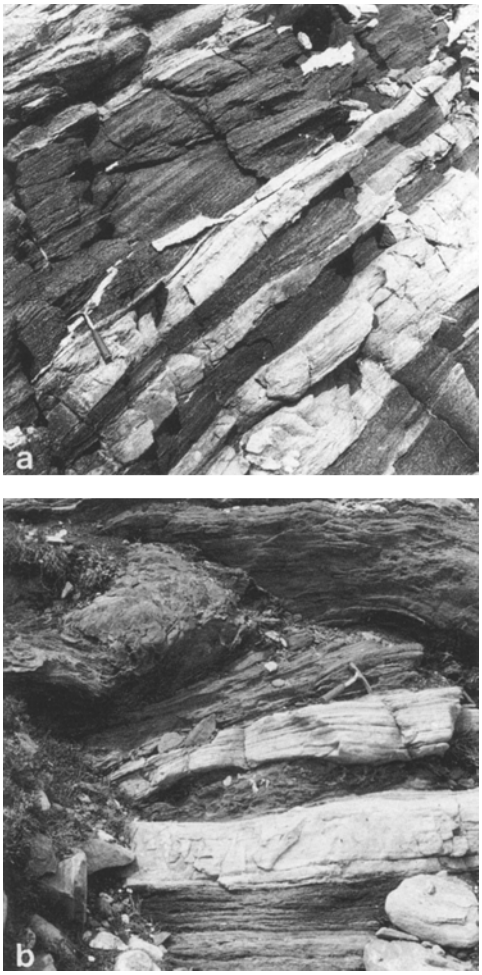

Fig. 2a, b. Field relations. **a** Blueschist unit, Vroulidia Bay, unit VR2: interlayering of blueschists (dark) and jadeite gneisses (light grey); **b** Greenschist layer Kamares Bay, unit K5: albite gneisses (light) interlayered with greenschists (dark grey); omphacite-rich eclogite relict is shown on *top left corner*

In the *Greenschist layers at Kamares Bay* rocks of chemical compositions equivalent to those of Vroulidia Bay (Table 1) are composed of albite + quartz + white mica in metasediments and meta-acidites and albite + epidote + chlorite + actinolite or calcite in the metabasites. In many samples, the development of reaction textures and the presence of relict minerals provide evidence for the earlier high-pressure metamorphic phase. As noted previously, relicts of omphacite-rich eclogites are occasionally well preserved. The development of greenschist facies assemblages is not accompanied by large chemical changes (Table 1). Only rocks of units K3 and K4, which are close to the marble contact, show enrichments in CaO which presumably reflect introduction of calcite. The similarities of the interlayering and the chemical compositions, and the evidence for the blueschist to greenschist facies transformation, clearly iden-

Table 1. Mineral assemblages and bulk-rock chemistries

	Blueschist unit, Vroulidia Bay										
	VR2						VR6	VR8			
wt%	76-311	84-71	84-73	77-312	84-72	84-74	600	76-290	77-569	84-78A	84-78B
SiO_2	74.4	78.0	71.2	51.7	48.5	47.5	54.6	46.5	45.0	44.9	44.2
TiO_2	0.25	0.17	0.23	1.17	0.66	0.65	1.16	0.72	0.65	0.65	0.73
Al_2O_3	12.0	11.7	14.1	16.1	16.0	14.7	15.4	12.7	11.0	10.0	11.1
Fe_2O_3	2.26	0.93	1.01	2.68	2.34	2.15	5.90	2.19	2.38	2.02	2.71
FeO	1.84	1.55	1.93	8.98	5.76	5.81	6.12	5.81	6.25	6.30	6.22
MnO	0.08	0.05	0.07	0.15	0.15	0.15	0.32	0.13	0.12	0.16	0.16
MgO	0.72	0.95	1.11	3.84	8.95	9.26	3.94	14.6	18.7	20.2	19.6
CaO	1.28	2.10	4.08	5.19	6.77	7.61	7.96	8.71	9.26	8.16	8.70
Na_2O	5.17	0.83	1.32	4.34	4.71	4.72	2.08	1.45	0.87	0.97	0.89
K_2O	0.31	2.55	2.18	0.32	0.39	0.36	0.56	1.21	0.11	0.47	0.15
P_2O_5	0.04	0.02	0.03	0.15	0.17	0.12	0.06	0.26	0.23	0.26	0.27
CO_2	0.6	0.1	1.2	2.8	2.6	3.5	0.25	1.2	0.05	0.55	0.15
H_2O	0.8	1.7	2.3	2.3	4.1	3.9	2.2	4.6	5.3	6.1	6.0
$\sum$	99.75	100.65	100.76	99.82	101.10	100.43	100.55	100.08	99.92	100.74	100.88
Quartz	●	●	●	○	+	+	+	+	–	–	–
Albite	+	+	+	–	–	–	–	–	–	–	–
Jadeite	○	+	+	–	–	–	–	–	–	–	–
Omphacite	–	–	–	–	–	–	–	–	–	–	–
White mica	○	○	○	●	+	○	○	○	–	○	○
Chlorite	–	+	–	+	+	+	+	○	●	●	●
Glaucophane	○	–	+	●	●	●	●	○	–	–	–
Actinolite	–	–	–	–	–	–	–	●	●	●	●
Garnet	○	○	○	●	○	○	○	–	–	–	–
Epidote	+	○	○	–	●	○	●	○	○	○	○
Sphene	–	–	–	+	+	+	–	○	+	+	+
Rutile	+	–	–	+	–	–	+	+	–	–	–
Calcite	○	–	+	○	○	○	–	○	–	+	–

● > 20, ○ 20-2, + < 2 vol. %

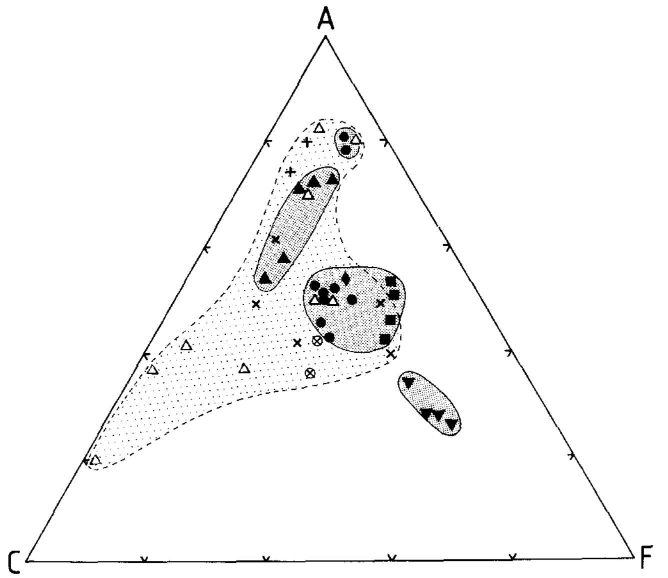

Fig. 3. $Al_2O_3+Fe_2O_3-FeO+MgO-CaO$ (*AFC*) triangular plot of whole-rock chemical compositions of blueschist (*heavily stippled*) and greenschist facies rocks (*light stippled areas*) from Vroulidia Bay, Kamares Bay and Central Sifnos. Data sources Table 1. Legend: see Fig. 9

tify the Kamares Bay sequence as being lithologically equivalent to the interlayered blueschist rocks of Vroulidia Bay.

Mineral assemblages of the *Greenschist unit of Central Sifnos* are typical of greenschist facies conditions. Relict high-pressure minerals such as glaucophane are often present as armoured inclusions in epidote or albite and occur most frequently in calcite-rich parageneses. All the examined rocks of this study contain varying amounts of calcite (Table 1). The chemical data plotted in Fig. 3 show that the compositions of the greenschist facies rocks of Central Sifnos vary from those of the original blueschist facies rocks towards the CaO apex. It is assumed that these trends represent the metasomatic introduction or remobilization of Ca^{2+}- and CO_2-bearing solutions into or within rocks that were originally similar in composition to the blueschist facies rocks of northern Sifnos. At the same time, water required for hydration reactions must have been introduced. On average the H_2O content of basic rocks increased by 1.2 wt% during the transformation from blueschist to greenschist facies assemblages (data in Table 1).

Mineral reactions in metabasic rocks

The transformation from blueschist to greenschist facies assemblages is best expressed by reactions occurring in metabasic rocks. A number of reactions can be observed in

Table 1 (continued)

Blueschist unit, Vroulidia Bay												
VR9		VR10			VR12							
84-79A	84-79B	76-241	76-565	76-566	76-94	76-95	76-96	76-97	76-100	84-62	84-63	84-64A
66.6	62.8	51.3	49.8	47.2	51.7	75.2	52.4	76.1	53.5	52.5	72.8	53.8
0.22	0.36	0.88	0.97	0.93	1.08	0.24	1.00	0.26	0.78	0.97	0.26	0.81
11.5	12.0	16.2	17.3	17.6	15.3	11.9	15.6	11.8	14.9	13.0	12.8	13.7
1.15	1.63	3.37	2.01	2.93	2.96	1.06	3.20	0.99	3.23	3.69	1.33	4.08
1.62	1.81	4.24	6.56	5.64	4.40	1.44	3.34	1.41	3.32	4.11	1.39	3.14
0.08	0.19	0.08	0.13	0.18	0.12	0.12	0.14	0.12	0.15	0.15	0.12	0.16
1.42	1.36	5.11	5.61	4.03	6.31	1.11	4.87	0.96	5.58	5.28	0.80	5.40
6.31	8.43	8.45	4.91	9.77	7.83	5.78	9.34	4.98	9.33	9.92	1.08	9.46
0.95	0.55	3.93	3.01	2.72	3.38	1.71	4.64	2.07	5.27	5.57	6.36	6.07
3.35	3.56	3.70	4.50	4.03	4.14	1.09	3.10	0.67	2.58	2.30	1.13	2.39
0.06	0.10	0.80	1.01	1.23	0.67	0.05	0.67	0.07	0.33	0.47	0.06	0.37
3.1	4.5	<0.1	1.1	2.0	<0.1	<0.1	<0.1	<0.1	<0.1	<0.1	<0.1	<0.1
2.3	2.3	1.6	2.7	2.2	2.0	1.0	1.5	0.9	1.2	1.1	0.8	1.2
98.66	99.56	99.66	99.61	100.46	99.89	100.70	99.80	100.33	100.17	99.06	98.83	100.58
●	●	+	−	−	−	●	−	●	−	+	○	+
−	−	−	−	−	−	+	−	+	−	−	○	−
−	−	−	−	−	−	○	−	○	−	−	●	−
−	−	●	+	●	●	−	●	−	●	●	−	●
●	●	●	●	●	●	○	●	○	●	○	○	○
−	+	−	−	−	+	−	−	+	−	−	−	−
○	+	○	●	○	○	+	−	−	−	−	+	−
−	−	−	−	−	−	+	−	−	−	−	−	−
○	○	○	○	○	○	○	○	○	○	+	−	−
○	○	+	+	○	−	●	○	●	+	+	+	+
+	+	+	○	+	+	+	+	+	+	+	−	+
−	−	−	−	−	−	−	−	−	+	−	−	−
○	○	−	○	○	−	−	−	−	−	−	−	−

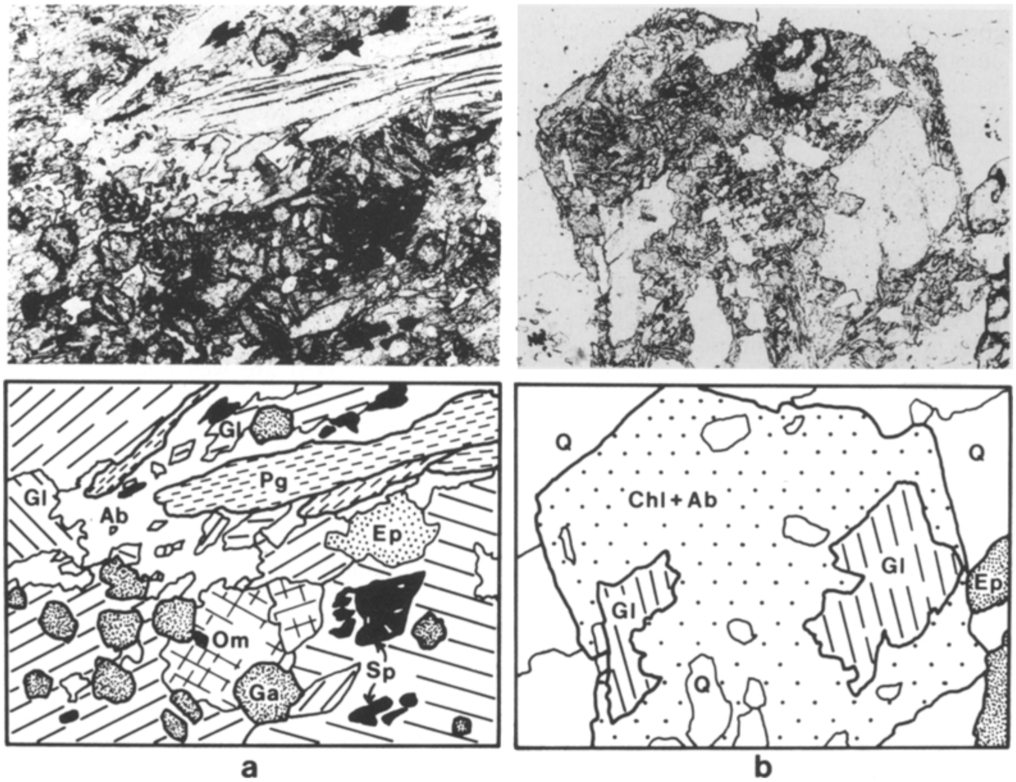

Fig. 4a, b. Photographs with accompanying sketch of **a** omphacite (*Om*) + paragonite (*Pg*) breakdown reaction to albite (*Ab*) + glaucophane (*Gl*) in rock Si 76-362. Also present are epidote (*Ep*), garnet (*G*) and sphene (*Sp*). **b** Glaucophane from rock Si 76-424 breaking down to chlorite + albite symplectite (*Chl* + *Ab*). Also present are epidote and quartz (*Q*). Photo widths are 1 mm

Table 1 (continued)

	Blueschist unit, Vroulidia Bay		Greenschist Layer, Kamares Bay								
	VR12		K3		K4				K5		
wt%	84-65	84-66	84-46A	84-52	84-47A	84-48A	84–48B	84-49	84-53	84-57	84-54
SiO_2	74.0	52.8	45.4	44.2	42.2	76.5	71.7	68.3	70.6	73.3	53.3
TiO_2	0.27	0.83	0.34	0.45	0.67	0.19	0.36	0.33	0.30	0.27	0.82
Al_2O_3	13.3	14.0	10.3	11.6	14.1	12.4	12.7	15.2	15.1	14.6	13.9
Fe_2O_3	0.63	2.27	1.39	3.00	6.08	1.69	2.42	2.47	2.15	1.83	3.76
FeO	1.46	4.72	0.59	1.69	1.57	0.78	1.28	1.78	0.72	0.91	4.26
MnO	0.07	0.15	0.08	0.10	0.09	0.05	0.10	0.08	0.05	0.06	0.12
MgO	0.88	6.21	0.54	1.88	4.10	0.62	1.28	1.27	0.87	0.85	8.15
CaO	3.17	10.4	19.0	18.0	15.0	1.64	1.11	4.60	2.80	4.09	6.29
Na_2O	1.74	5.36	0.28	2.15	1.98	3.83	2.04	1.57	5.04	3.25	3.93
K_2O	2.09	2.05	2.33	1.67	3.90	1.55	3.64	2.46	1.41	1.69	1.99
P_2O_5	0.01	0.11	0.13	0.15	0.08	0.05	0.11	0.07	0.05	0.05	0.41
CO_2	<0.1	<0.1	16.8	13.2	8.1	<0.1	<0.1	<0.1	0.15	0.15	0.35
H_2O	1.7	1.1	2.7	2.8	2.6	1.1	2.7	2.2	1.7	1.5	3.4
$\sum$	99.36	100.00	99.88	100.89	100.47	100.40	99.53	100.33	100.94	101.55	100.68
Quartz	●	–	●	○	+	●	○	○	○	○	+
Albite	–	–	○	○	○	●	○	○	●	●	○
Jadeite	–	–	–	–	–	–	–	–	–	–	–
Omphacite	–	●	–	–	–	–	–	–	–	–	–
White mica	○	○	○	○	●	○	●	○	○	○	○
Chlorite	–	–	○	○	–	+	+	○	○	+	○
Glaucophane	–	+	–	–	+	–	–	–	–	–	–
Actinolite	–	–	–	–	○	–	–	–	–	–	●
Garnet	○	○	–	+	–	+	+	+	+	–	–
Epidote	○	+	–	○	●	+	○	○	○	○	○
Sphene	+	+	–	+	+	–	–	–	+	–	+
Rutile	–	–	–	–	–	–	–	–	–	–	–
Calcite	–	–	●	●	○	–	–	–	–	–	+

thin sections. Two of these reactions, illustrated in Fig. 4a and b, show the breakdown of omphacite and glaucophane according to the reactions:

omphacite + paragonite → glaucophane + albite ± epidote

and

glaucophane ± epidote → chlorite + albite.

On the basis of the reactions that can be observed petrographically, it is possible to construct a reaction sequence for the blueschist-to-greenschist transformation in metabasic rocks (Fig. 5). All assemblages are projected from epidote, quartz, H_2O and CO_2 onto the $Al + Fe^{3+} - Na(Al + Fe^{3+}) - Ca(Mg + Fe^{2+})$ plane (Kohlmann and Schliestedt 1979). Blueschist facies parageneses are represented in Fig. 5a as three phase assemblages: Gl–Om–Act, Gl–Om–Pg, Gl–Pg–Ctd (for notation see caption to Fig. 5). Apparently crossing tie lines involving garnet are due to the combination of Fe^{2+} and Mg^{2+} in the diagram.

The transformation from blueschist to greenschist assemblages involves first the breakdown of omphacite-bearing assemblages followed by the disappearance of glaucophane (Fig. 5b, c). Greenschist facies assemblages (Fig. 5d) are represented by the parageneses Ab–Chl–Act and Ab–Act–Cc. Both parageneses are observed in the greenschists at Kamares Bay.

In greenschists close to the marble contact and in the greenschists of central Sifnos, actinolite is not found or is minor (Table 1). This is taken to reflect higher X_{CO_2} in the fluid phase (Harte and Graham 1975).

With one exception, the reaction sequence presented in Fig. 5 involves reactions of hydration and carbonation. The reaction processes are thus dependent on the availability of a fluid phase.

The $P-T$ conditions of the retrogressive reaction sequence are bounded by conditions for the equilibration of the blueschist and greenschist metamorphic assemblages. The $P-T$ conditions noted in the introduction (Blueschist unit: $460 \pm 30°$ C, $P_{fluid} = 15 \pm 3$ kb; Greenschist unit: ~ 400–$480°$ C, $P_{fluid} = \sim 4$–7 kb) are well constrained for the blueschist facies metamorphism, but less well defined for the greenschist facies metamorphism (cf., Matthews and Schliestedt 1984). In order to further constrain the physical conditions, we have calculated a number of $P-T-X_{CO_2}$ equilibria among phases involved in the blueschist-to-greenschist transformation. The calculations are made using the program THERM (kindly provided by Dr. T.J.B. Holland) which utilizes data from the recently published thermodynamic dataset of Holland and Powell (1985), augmented in the case of our calculations by unpublished data for glaucophane (T.J.B. Holland, personal communication). The calculations are of equilibria in the system $SiO_2 - Al_2O_3 - MgO - CaO - Na_2O - H_2O - CO_2$. Compositions of end-member phases and the stoichiometries of the se-

Table 1 (continued)

Greenschist Layer Kamares Bay			Greenschist unit, Central Sifnos					
K5								
84-58	77-534	84-55A	83-26	83-37	77-507	77-511	76-156	76-163
49.7	55.6	52.9	41.4	39.7	49.9	50.6	41.9	46.8
0.81	n.d.	0.66	0.61	0.08	0.74	0.64	0.96	0.86
13.6	9.1	11.9	12.5	4.67	17.3	16.3	15.1	18.0
2.42	4.2	3.46	2.46	2.11	0.82	1.12	2.08	8.90
5.18	3.0	2.54	3.18	0.50	6.55	5.76	5.20	1.32
0.14	0.1	0.11	0.11	0.02	0.08	0.10	0.14	0.13
10.8	7.8	7.22	3.86	0.30	2.67	2.70	4.65	3.23
7.95	13.3	11.1	17.9	27.4	8.52	8.96	14.0	12.2
2.36	7.0	4.36	2.91	0.86	2.47	2.23	3.31	2.64
1.97	n.d.	2.53	1.69	1.50	2.86	2.52	0.85	1.16
0.37	n.d.	0.50	–	–	0.31	0.21	0.16	0.13
0.4	n.d.	0.6	9.3	17.5	4.4	6.2	8.1	1.9
4.1	n.d.	2.0	4.2	5.5	3.2	3.3	3.5	2.3
99.80	100.1	99.98	99.67	100.14	99.82	100.64	99.95	99.57
+	–	–	+	+	+	○	+	+
○	+	+	○	+	●	●	●	●
–	–	–	–	–	–	–	–	–
–	●	●	–	–	–	–	–	–
○	+	○	○	○	○	●	○	○
○	–	+	○	+	○	○	●	○
–	–	–	–	–	–	–	+	○
●	+	○	–	–	–	–	+	–
–	–	+	–	–	–	–	–	–
○	+	○	○	+	○	○	○	●
+	+	+	+	+	+	+	+	+
–	–	–	–	–	–	–	–	–
+	+	+	●	●	○	●	●	○

lected equilibria are presented in Table 2. Although not strictly necessary from a thermodynamic point of view, the reactions are chosen so as to correspond to the chemographically deduced sequence of reactions shown in Fig. 5. The calculations are made for representative compositions of Sifnos mineral phases determined by microprobe analyses. These compositions are detailed in Table 2 together with appropriate activities of end-member components.

The calculated equilibria are presented in Fig. 6a on a $P-T$ diagram for the hydration reactions 1 to 4 in Table 2 at $X_{CO_2}=0$ and in Fig. 6b on a $P-X_{CO_2}$ diagram for reactions 4 to 6, assuming a representative temperature of 450° C. Approximate P-T conditions for the blueschist and greenschist metamorphism and the curve for the jadeite+quartz=albite reaction after Holland (1983) are also shown in Fig. 6a.

At 450° C all four hydration curves plotted in Fig. 6a group around 9 kb and are in good agreement with a recent experimental investigation of reaction 4 (Maruyama et al. 1986). The slopes of the curves are shallow and even a generous estimate on errors and temperature variations would give 10 to 8 kb as a reasonable estimate of pressure conditions at $X_{CO_2}=0$. The influence of X_{CO_2} variations is illustrated in Fig. 6b. The two hydration-carbonation reactions 5 and 6 are of a maximum type, whereas hydration reactions, such as 4, only show a significant pressure decrease at high X_{CO_2}. Thus, at pressures of around 9 kb the hydration equilibria are occurring over a wide range of X_{CO_2} and reactions such as 5 are only stable at low X_{CO_2}. Whereas the occurrence of lawsonite pseudomorphs and of H_2O-rich fluid inclusions point to very low X_{CO_2} conditions during the blueschist facies metamorphism, X_{CO_2} may have increased during the greenschist facies overprint as indicated by Chl–Cc–Ep assemblages (reaction 7, Fig. 6b). Without a more detailed study, it is impossible to make any more firm conclusions about X_{CO_2} conditions.

Stable isotope geochemistry

Oxygen isotope evidence for fluid infiltration

Matthews and Schliestedt (1984) based their arguments for the involvement of fluid infiltration in the blueschist-to-greenschist transition on the enrichment of ^{18}O of coexisting minerals in Central Sifnos greenschists compared to blueschists in northern Sifnos. Consequently, if movement of ^{18}O-enriched fluids occurred, the Kamares Bay greenschist facies layer should also show higher $\delta^{18}O$ compositions than found in the blueschists. We explore this possibility and the inferences of the oxygen isotope data for the mechanism of fluid infiltration by first considering $\delta^{18}O$ relationships between an interlayered eclogite-jadeite gneiss-metasediment sequence at Vroulidia Bay with a lithologically equivalent interlayering of greenschists (containing relict eclogites) and albite gneisses at Kamares Bay.

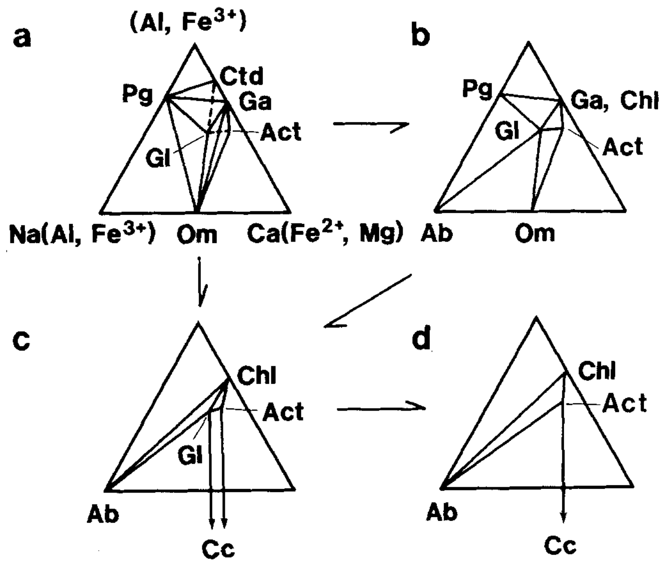

Fig. 5a–d. Petrographically deduced reaction sequence for the blueschist to greenschist facies transformation in metabasic rocks. The breakdown of blueschist facies assemblages (**a**) to form greenschist facies assemblages (**d**) is interpreted in terms of a chemographic sequence of reactions: (a) → (b) $Om+Pg=Ab+Gl+Ep+H_2O$, $Gl+Ctd+H_2O=Pg+Chl$; (a) → (c) $Om+Pg+H_2O=Ab+Chl+Ep$; (b) → (c) $Gl+Pg+H_2O=Ab+Chl+Q$, $Om+H_2O+CO_2=Ab+Chl+Cc+Ep$, $Ga+H_2O=Chl+Ep+Q$; (c) → (d) $Gl+Ep+H_2O=Ab+Act+Chl$. *Mineral abbreviations: Ab* albite; *Act* actinolite; *Cc* calcite; *Chl* chlorite; *Ctd* chloritoid; *Ep* epidote; *Ga* garnet; *Gl* glaucophane; *Om* omphacite; *Pg* paragonite; *Q* quartz

The relationships are described in Fig. 7. It is evident that the Kamares Bay greenschist and albite gneiss samples are 2–3‰ enriched in ^{18}O relative to equivalent eclogites and acidic rocks in the Blueschist unit. The lowest $\delta^{18}O$ values in the Kamares Bay layers occur in the partially overprinted eclogite samples, which have compositions 0.5 to 1.2‰ lower than in greenschists.

The data emphasize two critical aspects of the fluid-infiltration model: 1) the Kamares Bay samples show ^{18}O-enrichments relative to equivalent blueschist facies rocks in northern Sifnos, 2) the higher $\delta^{18}O$ of greenschists at Kamares Bay, compared to eclogites they enclose and from which they are derived, is consistent with the infiltration of ^{18}O-enriched fluids into this section.

Two other features evident in Fig. 7 are the homogeneity of isotopic compositions of samples within any particular layer of the Vroulidia Bay site (at least over the 5 m scale of sampling) and the fact that acidic rocks have much higher $\delta^{18}O$ compositions than basic rocks in the same section.

The isotopic compositions of rocks and minerals at equilibrium are dependent on their chemistry. Studies of fractionation (e.g., O'Neil and Taylor 1967; Wenner and Taylor 1971; Bottinga and Javoy 1973; Matthews et al. 1983) identify the importance of the $Si-O-Si$, $Si-O-Al$ and $Si-O-M^{2+}$ bonding in dictating the equilibrium isotopic compositions of minerals. In this respect the higher $\delta^{18}O$ values of the acidic relative to basic rocks are consistent with the known fact that the greater the SiO_2 content of a rock the greater its ability to concentrate ^{18}O (Taylor and Epstein 1962; O'Neil and Taylor 1967).

Several attempts have been made to interpret the oxygen isotopic compositional behaviour of rocks and minerals in terms of their chemical components (e.g., Garlick 1966; Broecker and Oversby 1971). The simplest is the empirical chemical index of Garlick (1966)

$$I=\frac{(Si+0.58\ Al)}{\Sigma \text{ cations}} \text{ oxygen equivalents.}$$

This index is plotted in Fig. 8 against the coefficients $A_{\text{Q-Mineral}}$ in the high-temperature mineral-mineral equilibrium relationship $1000 \ln\alpha=\Delta_{\text{Q-Mineral}}=A\times\frac{10^6}{T^2}$ where Q is quartz. The A coefficients used in Fig. 8 are taken from the calibrations presented in Matthews et al. (1983a, b) and Matthews and Schliestedt (1984). Excluding the points for calcite and rutile, all data fall on a reasonable linear relationship between A and I, which can be expressed by the regression equation

$$A_{\text{Q-Mineral}}=6.15\text{–}6.32\times I.$$

The minerals for which the linear relationships are observed include the components $Si-Al-K-Na-Fe^{2+}-Fe^{3+}-Mg-O-H$. Thus, to a first and surprisingly good approximation it appears that the isotopic behaviour of rocks and minerals at equilibrium will show a linear dependence on the Garlick index. The slope of a $\delta^{18}O$ vs. I plot will of course be dependent on the temperature at which the assemblages equilibrated. The major exception to the linear relationship is calcite which should be excluded from any plot. In practice this entails subtracting the $CaCO_3$ content of a rock from its whole-rock analysis prior to calculating I and correspondingly analyzing the isotopic compositions of a whole-rock sample from which carbonate has been removed (cf., Table 3).

Figure 9 plots the $\delta^{18}O$ compositions of whole-rocks from the three sample areas against the index I. Also represented on the diagram are isopleths showing the isotopic compositions of H_2O in equilibrium at an assumed representative temperature of 450° C (method of calculation is given in the caption to Fig. 9).

Both the Vroulidia Bay blueschist facies samples and the Kamares Bay greenschist facies rocks show linear trends which are sub-parallel to the isopleths of water composition. Waters in equilibrium with the blueschist facies samples mostly range from ~10 to 12‰, and in equilibrium with Kamares Bay greenschist facies samples from ~13.5 to 14.5‰. Thus, the interlayered rocks of both units appear to have experienced a substantial degree of isotopic equilibration. The smale-scale features noted in Fig. 7 are seen to reflect the general tendency of interlayered rocks to approach isotopic equilibrium during both the high-pressure metamorphism and the subsequent overprint. The two relict eclogite samples (50,534) from Kamares Bay plot within the general field of Vroulidia Bay compositions. A more overprinted eclogite sample (55A) is slightly enriched in $\delta^{18}O$ relative to Vroulidia samples, but still falls below the Kamares Bay greenschist facies field.

The Central Sifnos greenschists show a steeply trending variation of $\delta^{18}O$ with I. Sampling of this unit was distributed over a much wider area than in the other two units (see Matthews and Schliestedt 1984 for detailed locations) and, in the absence of a number of more acidic rock types, it is impossible to say whether any significant approach to isotopic equilibrium has occurred between the generally macroscopicly interlayered lithologies of this unit. Compositions of H_2O in equilibrium with the Central Sifnos samples vary from approximately 16–18‰.

Table 2. Details of the model reactions used in the $P-T-X_{CO_2}$ calculations of Fig. 6

	SiO_2	Al_2O_3	MgO	CaO	Na_2O	H_2O	CO_2
A Endmember compositions							
Jadeite (jd)	2	0.25	0.5	0.5	0.25	0	0
Diopside (di)	2	0	1	1	0	0	0
Glaucophane (gl)	8	1	3	0	1	1	0
Paragonite (pa)	3	1.5	0	0	0.5	1	0
Clinozoisite (cz)	3	1.5	0	2	0	0.5	0
Low albite (abl)	3	0.5	0	0	0.5	0	0
Clinochlore (clin)	3	1	5	0	0	4	0
Tremolite (tr)	8	0	5	2	0	1	0
Calcite (cc)	0	0	0	1	0	0	1
Quartz (q)	1	0	0	0	0	0	0

B Reaction stoichiometries[a]

(1) $2\ \mathrm{di}+11\ \mathrm{gl}+6\ \mathrm{pa}+8\ H_2O=28\ \mathrm{abl}+6\ \mathrm{clin}+1\ \mathrm{tr}$
(2) $1\ \mathrm{jd}+5\ \mathrm{gl}+3\ \mathrm{pa}+4\ H_2O=14\ \mathrm{abl}+3\ \mathrm{clin}$
(3) $5\ \mathrm{gl}+3\ \mathrm{pa}+4\ H_2O=13\ \mathrm{abl}+3\ \mathrm{clin}+1\ \mathrm{q}$
(4) $25\ \mathrm{gl}+6\ \mathrm{cz}+7\ \mathrm{q}+14\ H_2O=50\ \mathrm{abl}+9\ \mathrm{clin}+6\ \mathrm{tr}$
(5) $5\ \mathrm{gl}+2\ \mathrm{cz}+6\ H_2O+4\ CO_2=10\ \mathrm{abl}+3\ \mathrm{clin}+4\ \mathrm{cc}+7\ \mathrm{q}$
(6) $15\ \mathrm{gl}+4\ \mathrm{cz}+10\ H_2O+CO_2=30\ \mathrm{abl}+6\ \mathrm{clin}+3\ \mathrm{tr}+2\ \mathrm{cc}$
(7) $3\ \mathrm{tr}+2\ \mathrm{cz}+8\ H_2O+10\ CO_2=3\ \mathrm{clin}+10\ \mathrm{cc}+21\ \mathrm{q}$

C Representative mineral compositions and related activities[b]

Omphacite	$(Na_{0.53}Ca_{0.46})_{0.99}(Al_{0.44}Fe_{0.08}Fe_{0.10}Mg_{0.38})_{1.00}Si_{2.01}O_6$	$a_{jd}=0.44$[c] $a_{di}=0.38$[c]
Glaucophane	$(Na_{1.95}Ca_{0.07})_{2.02}(Mg_{2.01}Fe_{1.04})_{3.05}$ $(Al_{1.70}Fe_{0.25})_{1.95}(Al_{0.05}Si_{7.95})_8O_{22}(OH)_2$	$a_{gl}=0.18$[d]
Epidote	$Ca_{1.99}(Al_{2.34}Fe_{0.60}Mn_{0.01})_{2.95}Si_{3.05}O_{11}OH$	$a_{cz}=0.36$[e]
Paragonite	$(Na_{0.96}K_{0.06})_{1.02}(Al_{1.97}Fe_{0.03})_{2.00}$ $(Al_{1.03}Si_{2.97})_4O_{10}(OH)_2$	$a_{pa}=0.92$[f]
Albite	$(Na_{0.97}Ca_{0.01})_{0.98}(Al_{1.00}Si_{3.02})_{4.02}O_8$	$a_{ab}=0.99$[g]
Chlorite	$(Mg_{2.76}Mn_{0.02}Fe_{1.84})_{4.62}Al_{1.26}(Al_{1.03}Si_{2.97})_4O_{10}\ (OH)_4$	$a_{clin}=0.074$[d]
Actinolite	$(Ca_{1.74}Na_{0.33}K_{0.02})_{2.09}(Mg_{3.36}Fe_{1.24}Mn_{0.02}Al_{0.35}$ $Fe_{0.04})_{5.01}(Al_{0.21}Si_{7.79})_8O_{22}(OH)_2$	$a_{tr}=0.074$[d]

[a] Calculated with the program (T.J.B. Holland, personal communication)
[b] Calculated according to the program AX (T.J.B. Holland, personal communication)
[c] $a_{jd}=x_{jd}$; $a_{di}=x_{di}$
[d] Ideal mixing on sites
[e] $a_{cz}=(x_{Ca})^2\ (x_{Al,\ M1})$
[f] Solution model of Chatterjee and Flux (1986)
[g] Solution model of Newton and Haselton (1981)

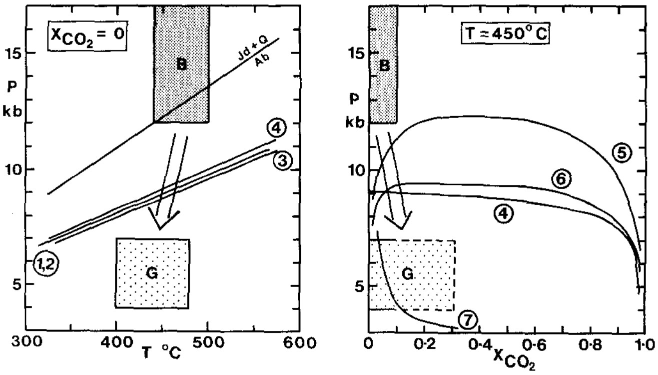

Fig. 6. $P-T$ and $P-X_{CO_2}$ plots showing schematic paths for the transition from blueschist facies (*heavily stippled*) to greenschist facies (*lightly stippled*) conditions. The following equilibria, calculated with the thermodynamic dataset of Holland and Powell (1985), are shown:
1 $2\ \mathrm{di}+11\ \mathrm{gl}+6\ \mathrm{pa}+8\ H_2O=28\ \mathrm{abl}+6\ \mathrm{clin}+1\ \mathrm{tr}$, *2* $1\ \mathrm{jd}+5\ \mathrm{gl}+3\ \mathrm{pa}+4\ H_2O=14\ \mathrm{abl}+3\ \mathrm{clin}$, *3* $5\ \mathrm{gl}+3\ \mathrm{pa}+4\ H_2O=13\ \mathrm{abl}+3\ \mathrm{clin}+1\ \mathrm{q}$, *4* $25\ \mathrm{gl}+6\ \mathrm{cz}+7\ \mathrm{q}+14\ H_2O=50\ \mathrm{abl}+9\ \mathrm{clin}+6\ \mathrm{tr}$, *5* $5\ \mathrm{gl}+2\ \mathrm{cz}+6\ H_2O+4\ CO_2=10\ \mathrm{abl}+3\ \mathrm{clin}+4\ \mathrm{cc}+7\ \mathrm{q}$, *6* $15\ \mathrm{gl}+4\ \mathrm{cz}+10\ H_2O+CO_2=30\ \mathrm{abl}+6\ \mathrm{clin}+3\ \mathrm{tr}+2\ \mathrm{cc}$, *7* $3\ \mathrm{tr}+2\ \mathrm{cz}+8\ H_2O+10\ CO_2=3\ \mathrm{clin}+10\ \mathrm{cc}+21\ \mathrm{q}$

The $\delta^{18}O$ compositional ranges of the three sample areas show a systematic increase from the lowest values in the Vroulidia Blueschist unit, to an intermediate range at Kamares Bay, and to the highest values of the (stratigraphically lowermost) samples in Central Sifnos. This inverse correlation of $\delta^{18}O$ with stratigraphy suggests the infiltration of ^{18}O-enriched fluids, which either decreased in $\delta^{18}O$ as the penetrated upwards or became volumetrically less adundant. The preservation of the blueschists in the upper levels of the stratigraphy suggests that these rocks did not experience much infiltration, i.e., fluids did not penetrate through to this unit. Fluid-rock ratios and the mechanisms of fluid movement will be discussed in detail shortly. The identification of ^{18}O-enriched fluids suggests that marbles were involved in the buffering of the isotopic compositions of the infiltrating solutions.

Isotopic compositional relations among marbles

The previous discussion has identified ^{18}O-enriched fluids in the blueschist-to-greenschist transition. The principal question adressed here is how the compositional relationships are expressed in marble units and carbonates occur-

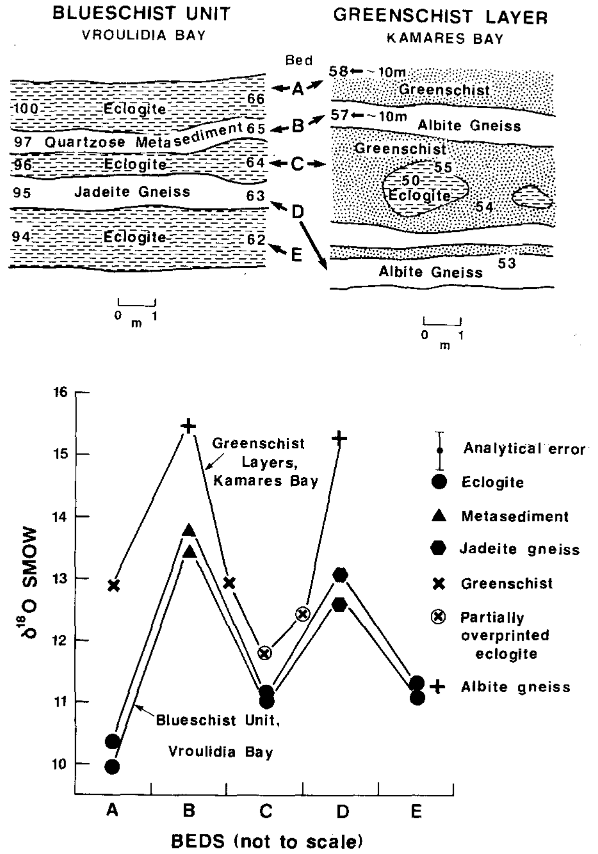

Fig. 7. Comparison of the isotopic compositional relationships of two interlayered units: an interlayered unit of blueschist facies acidic and basic rocks in Vroulidia Bay (Fig. 1, unit VR12) and a lithologically similar unit from the Kamares Bay section which has experienced the greenschist facies overprint (units K4 and K5, Fig. 1)

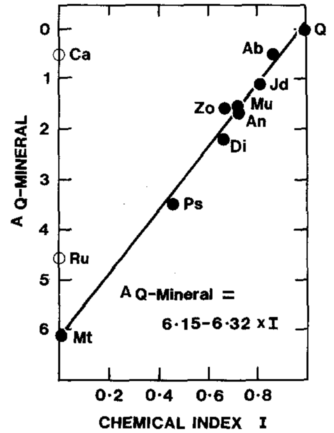

Fig. 8. Plot of Garlick chemical index *I* against $A_{\text{Q-mineral}}$ coefficients (see text for details)

ring within the three sample areas. Carbon and oxygen isotope analyses of calcium carbonates are presented in Table 3 and plotted in Fig. 10 on a $\delta^{13}C$ vs. $\delta^{18}O$ diagram.

The isotopic analyses can be loosely categorized into three groups: 1) High $\delta^{18}O$ (>24‰) and $\delta^{13}C$ (>0‰) samples of the Main and Upper Marble units (Fig. 1).

2) Low $\delta^{18}O$ compositions associated with carbonates of the blueschists ($\delta^{18}O = 13$ to 17‰) and greenschists (15 to 21‰).

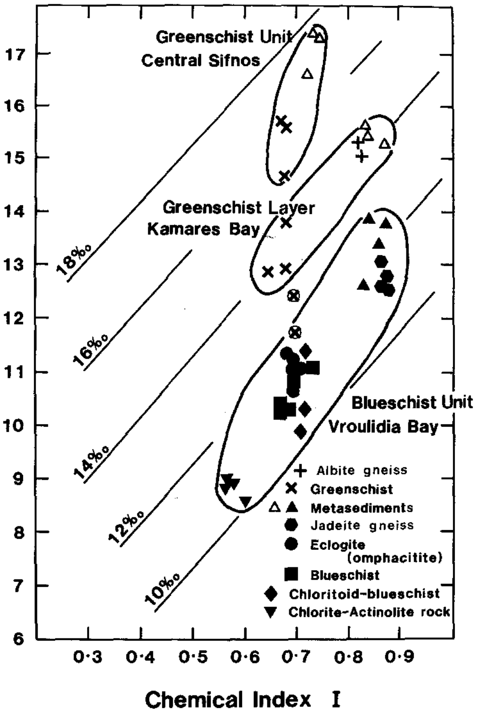

Fig. 9. Plot of $\delta^{18}O$ against chemical index *I* for whole rocks in the three sample areas. Isopleths showing water compositions in equilibrium with whole rocks at an assumed temperature of 450° C are obtained from the $A_{\text{Q-mineral}}$ vs. *I* relationship of Fig. 8 and the quartz-water calibration of Matsuhisa et al. (1979)

3) Low $\delta^{13}C$ (−6 to −12‰, $\delta^{18}O = 22$–25‰) compositions from calcite veins which cut all lithological units.

Within these three categories of carbonate compositions it is possible to discern several additional trends and distinctions. The Main Marble calcite samples have higher $\delta^{18}O$ compositions than Upper Marble samples. Both groups have isotopic compositions in the range of marine sedimentary carbonates. Carbonates within the blueschist facies assemblages are lower in $\delta^{18}O$ than those within greenschists. However both groups of carbonates show a similar trend of decreasing $\delta^{13}C$ and increasing $\delta^{18}O$ towards the low $\delta^{13}C$ compositions of the late vein group. This is consistent with the petrography, since both the blueschists and greenschists are frequently observed to contain small cross-cutting calcite veinlets. The isotopic trends can thus be viewed as arising from mixing of late carbonate vein compositions with blueschist and greenschist carbonate compositions of $\sim\delta^{18}O$, 13–15‰; $\delta^{13}C$, 0–2‰, and $\sim\delta^{18}O$, 15–18‰; $\delta^{13}C$, 0–2‰, respectively. These differences in $\delta^{18}O$ between the blueschist and greenschist facies carbonates parallel the differences between the silicate whole-rocks, and point to influences of the ^{18}O-rich fluid.

Isotopic compositions between those of the Main Marble and the greenschists are observed in the thin (~1 m) contact band of marbles occurring at the Kamares Bay contact (Fig. 10 and Fig. 1, unit K2). These transitional compositions must reflect a diffusional gradient between Main Marble compositions and those at greenschist values. Similar transitional compositional $\delta^{18}O$ zones have been observed at marble contacts within the high- and medium-grade schist sequences on Naxos (Rye et al. 1976). There does not appear to be any corresponding boundary zone in the adjacent schists of the Kamares Bay samples (Fig. 9).

Table 3. Isotope analytical results

Sample description and location		Carbonates		Silicates δ^{18}O SMOW[a] ‰	Chemical index I[a]
		δ^{13}C PDB ‰	δ^{18}O SMOW ‰		
Blueschist unit, north side of Vroulidia Bay					
Unit VR2 (Interlayered blueschist and jadeite gneisses)					
77-311A	Jadeite gneiss			12.80	0.875
84-71	Jadeite gneiss			12.62	0.878
84-73	Jadeite gneiss (10 m updip from 71)	−1.84	16.03	12.64	0.847
77-312A	Blueschist			11.08	0.730
84-72	Blueschist			10.47	0.668
84-74	Blueschist (10 m updip from 72)			10.40	0.668
Unit VR4 (Micaschists with calcite lenses)					
76-309B	Calcite lens	0.12	14.96		
84-758	Calcite lens	0.52	15.35		
84-75C	Calcite lens (100 m updip from 75B)	−0.15	16.04		
Unit VR6 (Chloritoid-bearing blueschist)					
84-600	Chloritoid-blueschist			11.48	0.718
Unit VR8 (Chlorite-actinolite schists)					
76-290	Chlorite-actinolite-rock			8.55	0.601
77-569	Chlorite-actinolite-rock			8.94	0.577
84-78A	Chlorite-actinolite-rock (at contact with mica-schist)			9.00	0.567
84-78B	Chlorite-actinolite-rock (0.5 m above 78A)			8.79	0.562
84-77A	Calcite vein (late)	−8.53	24.61		
84-77B	Calcite vein (late)	−8.55	24.73		
Unit VR9 (Garnet-micaschists)					
84-79A	Garnet-micaschist	−0.21	13.25	13.95	0.842
84-79B	Garnet-micaschist	−0.36	13.09	12.68	0.828
Unit VR10 (Phengite-rich eclogites with blueschists)					
76-241	Eclogite			10.68	0.701
76-565A	Mixed eclogite-blueschist			10.86	0.696
76-566A	Eclogite	−4.09	17.35	12.67	0.686
Unit VR12 (Interlayered eclogites (omphacitites) and quartzose metasediments)					
76-94	Eclogite			11.28	0.696
76-95	Jadeite gneiss			13.14	0.865
76-96	Eclogite			11.13	0.708
76-97	Quartz-metasediment			13.89	0.873
76-100	Eclogite			10.39	0.716
84-62	Eclogite (≙94; 7 m along strike)			11.04	0.708
84-63	Jadeite gneiss (≙95; 7 m along strike)			12.60	0.861
84-64A	Eclogite (≙96; 7 m along strike)			10.99	0.712
84-65	Quartz-metasediment (≙97; 7 m along strike)			13.46	0.862
84-66	Eclogite (≙100; 7 m along strike)			9.84	0.710
Greenschist facies layer in Main Marble, Kamares Bay					
Unit K1 (Main Marble)					
84-60A	Marble, ~15 m from contact	2.39	26.83		
84-60B	Marble, ~12 m from contact	2.27	27.29		
84-51A	Marble, contact	2.39	25.42		
Unit K2 (Contact zone marble)					
84-45	Pink marble at contact	2.29	23.93		
84-43B	Pink marble, ~5 cm from contact	−0.04	22.92		
84-43A	White calcite cutting 43B	1.52	23.90		
84-43C	White calcite cutting 43B	1.62	23.24		
84-51B	Marble, ~5 cm from contact	0.09	20.43		
84-51C	Marble, ~5cm from contact	0.88	23.72		
84-42B	Marble, ~50cm from contact	0.34	21.13		
84-42A	Vein cutting marble at 42	−8.04	24.83		
84-42C	Vein cutting marble at 42	−8.10	23.57		

Table 3 (continued)

Sample description and location		Carbonates		Silicates δ^{18}O SMOW[a] ‰	Chemical index I[a]
		δ^{13}C PDB ‰	δ^{18}O SMOW ‰		
Unit K3 (Micaschists)					
84-46A	Micaschist + contact zone marble	−2.44	21.64	15.65	0.838
84-52	Micaschist + contact zone marble	0.25	17.46	15.90	0.756
84-46B	Coarse vein cutting 46A	−7.57	23.62		
Unit K4 (Interlayering of greenschists with quartz-micaschists and albite gneiss)					
84-47A	Greenschist, ~3 m from contact	−1.41	18.96	13.87	0.681
84-47B	Calcite + galena vein cutting 47A	1.05	17.01		
84-48A	Quartz-micaschist			15.33	0.876
84-48B	Quartz-micaschist			15.48	0.837
84-49	Albite gneiss (= jadeite gneiss)			15.18	0.819
84-50A	Eclogite relict			11.76	0.720
Unit K5 (Interlayered albite gneisses and greenschists containing relict eclogite lenses)					
84-53	Albite gneiss			15.38	0.829
84-57	Albite gneiss			15.50	0.845
84-54	Greenschist			12.96	0.686
84-58	Greenschist			12.90	0.651
77-534	Eclogite relict			11.78	0.720
84-55A	Eclogite + greenschist + carbonate veins	−7.98	23.33	12.48	0.696
84-59	Calcite vein between 54 and 55A	−7.21	24.04		
Greenschist unit, Central Sifnos					
83-26	Greenschist, NE Artemon		16.93	15.69	0.676
83-37	Marble, W Kastro	1.40	15.60	16.64	0.722
77-507	Metasediment, W Kastro	0.27	18.21	17.49	0.732
77-511	Metasediment, W Kastro	−1.82	18.68	17.44	0.748
76-156	Greenschist, Katavati	0.20	16.59	14.64	0.683
76-163	Greenschist, Katavati	1.58	15.87	15.60	0.681
83-38	Matrix carbonate in greenschist, Kastro	2.09	15.96		
83-25	Matrix carbonate in greenschist, Artemon	−0.19	16.76		

[a] Values of the Chemical Index I (Garlick 1966) are calculated after subtraction of $\mathrm{CaO} \triangleq \mathrm{CO_2} = \mathrm{CaCO_3}$ from the whole-rock analyses. With the exceptions of sample 566A, all silicate whole-rock analyses were made on samples which had been acid-treated to remove coexisting carbonate or contained negligible carbonate

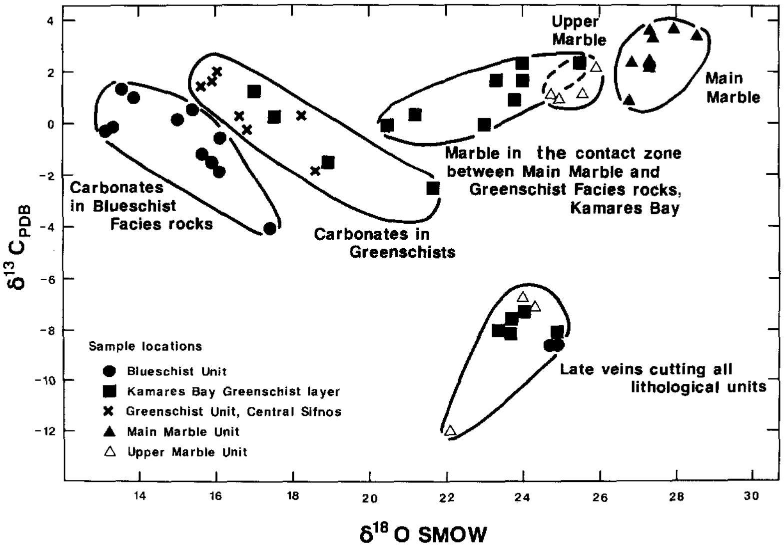

Fig. 10. δ^{13}C PDB vs. δ^{18}O SMOW plot of carbonates. *Data sources:* Table 3 and Matthews and Schliestedt (1984). Two samples (76-57, 83-Ky-27B) ascribed by Matthews and Schliestedt to the Upper Marble unit are considered here as belonging to the late veins on account of their petrography and low δ^{13}C

Transitional δ^{18}O values reflect diffusive broadening of sharp compositional contrasts occurring at marble-schist contacts as a result of advection (infiltration) (Bickle and McKenzie 1987). Diffusing CO_2 might have exchanged more readily with carbonates than silicates in this zone, bringing about late diffusive broadening after the passage of the main advection front.

The isotopic results for the carbonates clearly support the viability of marbles as the agents of buffering the carbon and oxygen isotopic compositions of the ^{18}O-enriched fluids. There is no evidence for the introduction of any exotic carbon component during the blueschist to greenschist facies transformation. Only in late veining is the presence of an exotic (and hitherto unidentified) isotopic component indicated.

Fluid-rock exchange systematics

Calculated oxygen isotope compositions of H_2O in equilibrium with whole-rocks at 450° C are (Fig. 9): Vroulidia Bay blueschists ~10–13‰, Kamares Bay ~13.5 to 15‰ and Central Sifnos ~16–18‰. If these gradients reflect upward movement of ^{18}O-enriched fluids, then the lower $\delta^{18}O$ values at Kamares Bay relative to Central Sifnos reflect either a) lowering of fluid/rock ratios as fluids moved upwards and/or b) isotopic compositions of fluids progressively decreased on upward movement as a result of exchange with silicates. The fact that blueschists are preserved in northern Sifnos is taken to mean that migrating fluids did not reach these units, i.e., it can be assumed that at the Main Marble-Blueschist unit contact (Fig. 1), the infiltrating-fluid/rock ratio is zero.

The suggestion (b), that the gradient is brought about simply as the result of progressive decrease in $\delta^{18}O$ during exchange appears untenable because it would require quite large fluid-rock ratios to occur at high levels in the Sifnos section. Additionally the fact that the fluid must see a lot of marble at all stratigraphic levels (the Kamares Bay section is enclosed by marble!) suggests that the fluids entering any level of silicate rocks will be enriched in ^{18}O prior to infiltration as a result of exchange with marbles. In other words, fluids decrease in $\delta^{18}O$ within silicate units as a result of fluid-rock exchange, but on, exiting from the silicate units, may subsequently be raised again in $\delta^{18}O$ as a result of exchange with marbles.

Minimum water/rock ratios can be calculated for the Kamares Bay and Central Sifnos greenschists by assuming that the initial fluids entering the zones had their $\delta^{18}O$ buffered at equilibrium with marble. The average $\delta^{18}O$ of the Main Marble is ~27.4‰ and, using the calcite-water equation of O'Neil et al. (1969), a $\delta^{18}O^i(H_2O)$ of 25‰ is calculated. Water-rock (W/R) ratios are calculated using the open-system (single pass) equation of Taylor (1977):

$$\frac{(\delta^{18}O^f-\delta^{18}O^i)_{\mathrm{rock}}}{(\delta^{18}O^i-\delta^{18}O^f)_{\mathrm{water}}}=\exp\,(W/R)-1$$

where the superscripts i and f refer to the initial and final states. The calculations are made using rocks of metabasic composition. Initial compositions are assumed as at Vroulidia, where a mean $\delta^{18}O^i(\mathrm{rock})=10.8‰$ is calculated from the data in Table 3. Corresponding calculated final conditions at Kamares Bay are $\delta^{18}O^f(\mathrm{rock})=13.2‰$, $\delta^{18}O^f(H_2O)$ at 450° C = 13.8‰ and in Central Sifnos, $\delta^{18}O^f(\mathrm{rock})=15.3‰$, $\delta^{18}O^f(H_2O)=15.9‰$. The resulting open-system water-rock atomic percent oxygen ratios are 0.2 for Kamares Bay greenschists and 0.4 for Central Sifnos. Since these ratios are expressed in atomic percent ratios they are also total fluid-rock ratios and independent of X_{CO_2}, provided that any CO_2 was also initially at equilibrium with the marble and remained at equilibrium with H_2O during exchange.

The calculations are of minimum fluid-rock ratios and ratios would, for instance, be larger if the initial water compositions were lower than the assumed value. On the other hand it must be recognized that we are arguing that the buffering of the initial compositions of the infiltrating fluid is a local process (i.e., within or adjacent to present Sifnos units). This raises the possibility that some local recycling of fluids may have occurred across contacts between marbles and schists, and consequently that lower amounts of fluid could have been involved.

The isotopic data has identified the history of the component of fluid flow upward through the stratigraphy. Flow of fluids along the strike of silicate units parallel to the concordant contacts between silicate units and marbles must also have occurred and, if the units were inclined as at present, brought about both dispersion and additional upward movement of fluids normal to the stratigraphy. Consumption of H_2O and CO_2 during the blueschist-to-greenschist reactions could also have contributed to the decrease in fluid/rock ratios. As noted, the average increase of H_2O content in metabasic rocks is 1.2 wt%. Compared to water/rock weight percent ratios (assuming all fluid were water) of ca. 0.1 (Kamares) and 0.2 (Central Sifnos) it is clear that the progressive removal of the fluid phase during hydration reactions could have occurred as fluids infiltrated.

Conclusions

Petrological and isotope studies have shown that the transformation of blueschist to greenschist facies assemblages on Sifnos occurred as a consequence of the infiltration of ^{18}O-enriched fluids whose initial isotopic compositions were buffered by exchange with marbles. The retrogressive processes represent the isothermal decompression stages of a broad clockwise $P-T$ loop (Matthews and Schliestedt 1984; Schliestedt et al. 1987) whereby blueschist assemblages formed at 460±30° C, 15±3 kb were transformed into greenschist assemblages at pressures of 10 to 8 kb. The transformation involved extensive hydration and carbonation for which the introduction of a fluid is necessary. Calculated single-pass minimum fluid-rock atomic percent oxygen ratios are 0.2 (Kamares Bay) and 0.4 (Central Sifnos), though the fact that extensive buffering of the ^{18}O of the fluids could have occurred locally allows for the possibility of lower fluid rock ratios, if recycling occurred across marble-schist contacts.

Fluid infiltration in prograde metamorphism is frequently associated with the occurrence of devolatization equilibria. Negative ΔV_S and positive overall volume changes (ΔV_R) on fluid release are considered to facilitate the effective mobilization of fluids (Rumble et al. 1982). On Sifnos fluid infiltration occurred in a relatively high-pressure hydration/carbonation reaction setting, where both the ΔV_R and ΔV_S terms may be positive (e.g., the hydration reactions of Fig. 6a). The available pore-space for fluid movement would therefore decrease as reactions proceed as a consequence of the volume filling. Infiltration would become inhibited as the transformation advanced. More complete reaction would be favoured for the earlier reacting omphacite-bearing assemblages than the later reacting glaucophane-bearing assemblages (Fig. 5). This indeed is the general observation on Sifnos where glaucophane-epidote is the most commonly preserved relict assemblage.

Transformation from high-pressure blueschists to medium-pressure greenschists is regionally typical of the Cycladean evolution. In this context, the relatively low amounts of fluid calculated for the Sifnos infiltration are appropriate. The fluids must be presumed to have come from a source which is either deeper-seated dehydrating metamorphic rocks or a crystallizing magma. In either case there is probably not enough fluid available to maintain high fluid/rock ratios of regional extent.

Acknowledgements. We would like to express our gratitude to Tim Holland for providing his thermodynamic calculating programs and for his criticisms when we used them. Reviews of Bernard Evans and Steve Wickham were also very helpful in preparing the final version of the paper. Shmuel Marco performed many of the oxygen isotope analyses and Marlies Korn kindly typed several versions of the manuscript. The research was supported by a grant from the Niedersächsische Minister für Wissenschaft und Kunst.

References

Bebout GE, Carlson WD (1986) Fluid evolution and transport during metamorphism: evidence from the Llano uplift, Texas. Contrib Mineral Petrol 92:518–529

Bickle MJ, McKenzie D (1987) The transport of heat and matter by fluids during metamorphism. Contrib Mineral Petrol 95:384–392

Bottinga Y, Javoy M (1973) Comments on oxygen isotope geothermometry. Earth Planet Sci Lett 20:250–265

Broecker WS, Oversby VM (1971) Chemical equilibria in the Earth. McGraw-Hill, New York, p 318

Chatterjee ND, Flux S (1986) Thermodynamic mixing properties of muscovite-paragonite crystalline solutions at high temperatures and pressures and their geological applications. J Petrol 27:677–693

Ferry JM (1983) Regional metamorphism of the Vassalboro Formation, south-central Maine, USA: a case study of the role of fluid in metamorphic petrogenesis. J Geol Soc London 140:551–576

Garlick GD (1966) Oxygen isotope fractionation in igneous rocks. Earth Planet Sci Lett 1:361–368

Graham CM, Greig KM, Sheppard SMF, Turi B (1983) Genesis and mobility of the H_2O-CO_2 fluid phase during regional greenschist and epidote amphibolite facies metamorphism: a petrological and stable isotope study in the Scottish Dalradian. J Geol Soc London 140:577–599

Greig KM, Graham CM, Fallick AE (1986) Stable isotope characterisation of fluid infiltration during prograde and retrograde regional metamorphism. Terra Cognita 6:210

Harte B, Graham CM (1975) The graphical analysis of greenschist to amphibolite facies mineral assemblages in metabasites. J Petrol 16:347–370

Holland TJB (1983) The experimental determination of activities in disordered and short-range ordered jadeitic pyroxenes. Contrib Mineral Petrol 82:214–220

Holland TJB, Powell R (1985) An internally consistent thermodynamic dataset with uncertainties and correlations. 2. Data and results. J Metamorph Geol 3:343–370

Kohlmann A, Schliestedt M (1979) Retrograde Mineralreaktionen in hochdruckmetamorphen Metabasiten der Inseln Sifnos und Tinos. Fortschr Mineral 57:68–69

Maruyama S, Liou JG, Cho M (1986) Experimental study on the blueschist-greenschist transition. Geol Soc Am Mem 164:1–17

Matsuhisa Y, Goldsmith JR, Clayton RN (1979) Oxygen isotope fractionation in the system quartz-albite-anorthite-water. Geochim Cosmochim Acta 43:1131–1140

Matthews A, Schliestedt M (1984) Evolution of the blueschist and greenschist facies rocks of Sifnos, Cyclades, Greece. A stable isotope study of subduction-related metamorphism. Contrib Mineral Petrol 88:150–163

Matthews A, Goldsmith JR, Clayton RN (1983a) Oxygen isotope fractionations involving pyroxenes: the calibration of mineral-pair geothermometers. Geochim Cosmochim Acta 47:631–644

Matthews A, Goldsmith JR, Clayton RN (1983b) Oxygen isotope fractionations between zoisite and water. Geochim Cosmochim Acta 47:645–654

Newton RC, Haselton HT (1981) Thermodynamics of the garnet-plagioclase-Al_2SiO_5-quartz geobarometer. In: Newton RC, Nawrotsky A, Wood BJ (eds) Thermodynamics of minerals and melts. Springer, Berlin Heidelberg New York, pp 131–147

O'Neil JR, Taylor HP (1967) The oxygen isotope and cation exchange chemistry of feldspars. Am Mineral 52:1414–1437

O'Neil JR, Clayton RN, Mayeda TK (1969) Oxygen isotope fractionation in divalent metal carbonates. J Chem Phys 51:5547–5558

Rumble D III, Ferry JM, Hoering TC, Boucot AJ (1982) Fluid flow during metamorphism at the Beaver Brook fossil locality, New Hampshire. Am J Sci 282:886–919

Rye RO, Schuiling RD, Rye DM, Jansen JBH (1976) Carbon, hydrogen and oxygen isotope studies of the regional metamorphic complex at Naxos, Greece. Geochim Cosmochim Acta 40:1031–1049

Schliestedt M (1980) Phasengleichgewichte in Hochdruckgesteinen von Sifnos, Griechenland. Ph D thesis, Technische Universität Braunschweig, p 142

Schliestedt M (1986) Eclogite-blueschist relationships as evidenced by mineral equilibria in high-pressure metabasic rocks of Sifnos (Cycladic islands) Greece. J Petrol 27:1437–1459

Schliestedt M, Okrusch M (1987) Meta-acidites and silicic metasediments related to eclogites and glaucophanites in northern Sifnos, Cycladic archipelago, Greece. In: Smith DC (ed) Developments in petrology: eclogites and eclogite-facies rocks. Elsevier, Amsterdam

Schliestedt M, Altherr R, Matthews A (1987) Evolution of the Cycladic crystalline complex: petrology, isotope geochemistry and geochronology. In: Helgeson HC (ed) Chemical transport in metasomatic processes (in press)

Taylor HP (1977) Water/rock interactions and the origin of H_2O in granitic batholiths. J Geol Soc London 133:509–558

Taylor HP, Epstein S (1962) Relationship between O^{18}/O^{16} ratios in coexisting minerals of igneous and metamorphic rocks. Part I. Principles and experimental results. Bull Geol Soc Am 73:461–480

Wenner DB, Taylor HP (1971) Temperature of serpentinization of ultramafic rocks based on $^{18}O/^{16}O$ fractionations between serpentine and magnetite. Contrib Mineral Petrol 32:165–185

Wickham SM, Taylor HP (1985) Stable isotope evidence for large-scale seawater infiltration in a regional metamorphic terrane; the Trois Seigneurs Massif, Pyrenees, France. Contrib Mineral Petrol 91:122–137

Received February 5, 1987 / Accepted June 2, 1987